



CHAPTER III

ULTRAFINE ELECTROSPUN POLYAMIDE-6 FIBERS: EFFECT OF SOLUTION CONDITION ON MORPHOLOGY AND AVERAGE FIBER DIAMETER

ABSTRACT

In the present contribution, the electrostatic spinning or electrospinning technique was used to produce ultra-fine polyamide-6 (PA-6) fibers. The effects of solution conditions on morphological appearance and average diameter of the as-spun fibers were investigated by optical scanning (OS) and scanning electron microscopy (SEM) techniques. It was shown that the solution properties (i.e. viscosity, surface tension, and conductivity) were important factors characterizing the morphology of the fibers obtained. Among the three properties, solution viscosity was found to have the greatest effect. The solutions with high enough viscosities (viz. solutions at high concentrations) were necessary to produce fibers without beads. At a given concentration, fibers obtained from PA-6 of higher molecular weights appeared to be larger in diameter, but it was observed that the average diameters of the fibers from PA-6 of different molecular weights had a common relationship with the solution viscosities which could be approximated by an exponential growth equation. Raising the temperature of the solution during spinning resulted in the reduction of the fiber diameters with higher deposition rate, while mixing *m*-cresol with formic acid to serve as a mixed solvent for PA-6 caused the solutions to have higher viscosity which resulted in the observed larger fiber diameters. Lastly, addition of some inorganic salts resulted in an increase in the solution conductivity, which caused the fiber diameters to increase due to the large increase in the mass flow.

KEY-WORDS: electrospinning process; ultrafine fibers; polyamide-6

1. INTRODUCTION

High electrostatic fields have wide applications in the industries.^[1] High electrostatic fields can be applied to either polymer solutions or melts to produce non-woven webs of ultrafine fibers, the diameters of which are in the range of few nanometers to sub-micrometers.^[2-6] Such a technique is called electrostatic spinning or electrospinning. Due to the exceptionally high surface area to mass ratio of the obtained fibers and the high density of pores in sub-micrometer length scale of the obtained non-woven webs, proposed applications for electrospun products are in areas where these properties are fully utilized. Some of the proposed applications for these products are, for examples, filters for separation of sub-micron particles, reinforcing fillers in composite materials, wound-dressing and tissue scaffolding materials for medical uses, and controlled release materials for agricultural and pharmaceutical uses.^[7]

Set-up of the electrospinning process is very simple. The three major components are a high-voltage power supply, a container for a polymer solution or melt with a small opening to be used as a nozzle, and a conductive collection device. An emitting electrode of the high-voltage power supply charges the polymer solution or melt by either directly submerging the electrode in the polymer solution or melt or by connecting the electrode to a conductive nozzle. The other or grounding electrode of the high-voltage power supply is connected to the conductive collection device to complete the circuit. Other set-ups are also possible.^[7] The Coulombic repulsion force between charges of the same polarity produced in the polymer solution or melt by the emitting electrode destabilizes the hemi-spherical droplet of the polymer solution or melt located at the tip of the nozzle to finally form a droplet of a conical shape (i.e. the Taylor cone). With further increase in the electrostatic field strength beyond a critical value, the Coulombic repulsion force finally exceeds that of the surface tension which finally results in the ejection of an electrically charged stream of the polymer solution or melt (i.e. the charged jet).

There are six major forces acting on an infinitesimal segment of the charged jet: they are 1) body or gravitational force; 2) electrostatic force which carries the charged jet from the nozzle to the target; 3) Coulombic repulsion force which tries to push apart adjacent charged species being present within the jet segment and is

responsible for the stretching of the charged jet during its flight to the target; 4) viscoelastic force which tries to prevent the charged jet from being stretched; 5) surface tension which also acts against the stretching of the surface of the charged jet; and 6) drag force from the friction between the charged jet and the surrounding air.^[8] Due to the combination of these forces, the electrically charged jet travels in a straight trajectory for only a short distance before undergoing a bending instability, which results in the formation of a looping trajectory.^[9,10] During its flight to the collector, the charged jet thins down and, at the same time, dries out or solidifies to leave ultrafine fibers on the collective screen.

In the electrospinning process of a polymer solution, a number of parameters can influence the morphology of the obtained fibers. These governing parameters can be categorized into three main types: 1) solution (e.g. concentration, viscosity, surface tension, and conductivity of the polymer solution); 2) process (e.g. applied electrostatic potential, collection distance, and feed rate); and 3) ambient parameters (e.g. temperature, relative humidity, and velocity of the surrounding air in the spinning chamber).^[7,11] Baumgarten^[12] was one of the early researchers who recognized the effects of some of these parameters on the morphological appearance of as-spun acrylic fibers. He found that an increase in the solution viscosity (as a result of an increase in the solution concentration) was responsible for an increase in the average fiber diameter, while an increase in the flow rate of the acrylic solution did not appreciably affect the fiber diameters.^[12]

Fong and co-workers^[13] investigated the formation of minute beads along the electrospun poly(ethylene oxide) (PEO) fibers by relating the phenomenon to the properties of the solutions. They found that the number of beads decreased with increasing viscosity and net charge density, while it decreased with decreasing surface tension coefficient, of the solutions.^[13] Deitzel and co-workers^[14] studied the effects of accelerating voltage and solution concentration on morphological appearance of electrospun PEO fibers. Buchko and co-workers^[15] found that the morphology of the electrospun protein non-woven webs depended on solution concentration, applied electric field strength, deposition distance, and deposition time. Demir and co-workers^[16] found that the average diameter of electrospun fibers from polyurethaneurea copolymer increased with the third power of the solution

concentration. Zong and co-workers^[17] found that solution concentration and addition of ionic salts had stronger effects on the morphological appearance of electrospun poly(D,L-lactic acid) (PDLA) and poly(L-lactic acid) (PLLA) fibers than other parameters. Choices of solvent or a combination of solvents used were also found to have a significant effect on the morphology of the electrospun fibers.^[8,18,19]

Although it has been shown in a recent review by Huang and co-workers^[7] that various aspects of electrospun fibers have been intensely explored and reported in the open literature in the past years, a number of fundamental aspects of the process for different polymer-solvent systems are still worthy of further investigation in order to gain a thorough understanding of the process. In the present contribution, the effects of various solution conditions (i.e. concentration, viscosity, surface tension, solution temperature, average molecular weight of the polymer, and addition of ionic salt) on morphological characteristics of electrospun polyamide-6 (PA-6) fibers were investigated using optical scanning (OS) and scanning electron microscopy (SEM) techniques.

2. EXPERIMENTAL DETAILS

2.1. Preparation and characterization of polyamide-6 solutions

Three fiber spinning grades of polyamide-6 (PA-6) (i.e. AFC-2002, AFC-2001, and AFC-3003) were supplied by Asia Fiber Public Co., Ltd. (Thailand). The weight-average molecular weights for these resins were reported to be 17,000, 20,000, and 32,000 Da, respectively. From this point forward, these resins will be called PA-6-17, PA-6-20, and PA-6-32, respectively. Solutions for electrospinning were prepared by dissolving each resin in a specified amount in formic acid (85% v/v, Carlo Erba). Slight stirring was used to expedite dissolution. Solutions of varying concentrations (i.e. 10 to 46% w/v for PA-6-17 and PA-6-20 resins and 10 to 34% w/v for PA-6-32 resin) were used to elucidate the effects of solution concentration and average molecular weight of PA-6 on morphological appearance of the obtained fibers. Various ionic salts (i.e. NaCl, LiCl, and MgCl₂) in various amounts were added in a PA-6 solution of specified concentration in order to investigate the effect of ionic salt addition on morphological appearance of the as-spun fibers. The effect of solvent system on the obtained fibers was studied by using

a mixture of formic acid and *m*-cresol in various volumetric ratios to prepare PA-6 solutions. A Brookfield DV-III programmable viscometer, a Krüss K10T tensiometer, and a Orion 160 conductivity meter were respectively used to measure viscosity, surface tension, and conductivity of the as-prepared solutions at room temperature (i.e. ca. 30°C) prior to electrospinning.

2.2. Set-up of electrospinning process

A 50-ml glass syringe was used to stock each of the as-prepared PA-6 solutions. A 1 cm-long stainless steel needle (gauge number 26), with a flat tip, was used as a nozzle. Both the syringe and the nozzle were tilted approximately 10° from a horizontal baseline in order to maintain a hemispherical droplet at the tip of the nozzle. The feed rate of PA-6 solutions was controlled by pressurized nitrogen gas through a flow meter. A piece of thick aluminum (Al) sheet was used as a collective screen. A Gamma High Voltage Research ES30P power supply was used to charge the spinning PA-6 solutions by connecting the emitting electrode of positive polarity to the nozzle and the grounding electrode to the collective screen. The distance between the tip of the nozzle and the collective screen defines a collection distance. In this particular work, a fixed electrostatic DC potential of 21 kV was applied over a fixed collection distance of 10 cm. Normally, the spinning solutions were kept at room temperature (i.e. 30°C), but, in order to study the effect of solution temperature on morphological appearance of the as-spun fibers, solutions of an elevated temperature (i.e. 40, 50, or 60°C) could be prepared by using a home-made double-chambered syringe, in which the outer chamber was circulated with warm water of a specified temperature.

2.3. Characterization of as-spun PA-6 fibers

The morphological appearance of the as-spun PA-6 fibers was investigated visually from optical scanning photographs of the as-spun webs collected on Al sheets using a 1200CS BearPaw optical scanner (OS) and from scanning electron micrographs of a small section of the same webs using a JEOL JSM-4200 scanning electron microscope (SEM). The specimens for SEM observation were prepared by

cutting an Al sheet covered with the as-spun webs and the cut section was carefully affixed on a SEM stub. Each specimen was gold-coated using a JEOL JFC-1100E sputtering device before being observed under SEM. For each spinning condition, at least 80 measurements for the fiber diameter were recorded. Statistical analysis of the data obtained was carried out by constructing a histogram, from which an arithmetic mean and a standard deviation were obtained and reported.

3. RESULTS AND DISCUSSION

3.1. Effect of PA-6 concentration on physical properties of as-prepared solutions

Solutions of all PA-6 resins in 85% v/v formic acid were prepared in various concentrations, ranging from 10 to 46% w/v for PA-6-17 and PA-6-20 and from 10 to 34% w/v for PA-6-32. The maximum of 34 wt.% for PA-6-32 was attained because the solutions prepared at higher concentrations were too viscous. Figure 1 shows the viscosity, surface tension, and conductivity values for solutions of PA-6 resins in 85% v/v formic acid as a function of PA-6 concentration. The viscosity values for solutions of all PA-6 resins were found to increase with increasing PA-6 concentration, with the values for PA-6-32 being much greater than those for PA-6-17 and PA-6-20 which, at a given concentration, were found to be very comparable to each other. Specifically, the values for PA-6-17 and PA-6-20 were found to monotonically increase from ca. 40 cp at 10% w/v to ca. 4000 cp at 46% w/v, while the value for PA-6-32 was found to monotonically increase from ca. 40 cp at 10% w/v to ca. 7000 cp at 34% w/v (see Figure 1a). The relationship between the solution viscosity and the solution concentration for all PA-6 resins could be approximated with an exponential growth equation (see equations in Figure 1a). The selection of the exponential growth equation to describe the data was based solely on the quality of the fitting that the equation provided.

The surface tension values for solutions of all PA-6 resins were found to monotonically increase but slightly with increasing PA-6 concentration. Specifically, the values for all of the solutions investigated were found to range between ca. 42 and 45 mN/m (see Figure 1b). The conductivity values for solutions of all PA-6 resins were found to increase initially to reach a maximum at a concentration of around 16 to 18% w/v and decrease with further increase in the

concentration of the solutions. Specifically, the values for all of the solutions studied ranged between ca. 3.3 and 4.6 mS/cm. The results obtained illustrate that an increase in the PA-6 concentration resulted in a significant increase in the viscosity, a slight increase in the surface tension, and a slight decrease in the conductivity of the resulting solution and that the viscosity of the resulting solution increased appreciably with increasing molecular weights of the dissolved polymer, while both the surface tension and the conductivity values were relatively less affected. The significant increase in the viscosity of the solutions with increasing PA-6 concentration is obviously due to the increased molecular entanglements.

3.2. Effect of PA-6 concentration

Figure 2 shows a selected series of scanning electron micrographs in order to illustrate the effect of the concentration of PA-6-17 solutions on morphological appearance of the obtained as-spun materials. At low concentrations (i.e. from 10 to ca. 18% w/v) or low viscosities (i.e. 39.2 to 157 cp), a large number of sub-micron droplets were present (see Figure 2a). At such low viscosities, the viscoelastic force (i.e. a result of the low degree of chain entanglements) in a given jet segment was not large enough to counter the higher Coulombic force, resulting in the break-up of the charged jet into smaller jets, which, as a result of the surface tension, were later rounded up to form droplets. This phenomenon has been familiarized in the industries as the electrospraying process and has commonly been used in many applications such as paint spraying, ink-jet printing, and powder coating, etc.^[1]

At higher concentrations or higher viscosities, the charged jet did not break up into small droplets, a direct result of the increased chain entanglements (i.e. hence an increase in the viscoelastic force) that were sufficient to prevent the break-up of the charged jet and to allow the Coulombic stress to further elongate the charged jet during its flight to the grounded target which ultimately thinned down the diameter of the charged jet.^[15] However, if the concentration was not high enough (e.g. 20% w/v), a combination of smooth fibers and minute, discrete droplets was obtained (see Figure 2b). A slight increase in the concentration of the solution to 22% w/v (or the viscosity of 277 cp) resulted in the disappearance of the minute, discrete droplets, leaving only a combination of smooth and beaded fibers on the target. With further

increasing concentration (or viscosity) of the solution, the number of beads along the fibers was found to decrease and their shape appeared to be more elongated (see Figure 2c and d). When the concentration of the solution was increased to 34% w/v (or the viscosity of 1332 cp), beads disappeared altogether, leaving only smooth ultrafine fibers on the target.

The formation of beads along the as-spun fibers could be a result of a number of different phenomena. For examples, it could be a result of the viscoelastic relaxation and the work of the surface tension upon the reduction of the Coulombic force once the fibers are in contact with the grounded target that drives the formation of the beads.^[13] This phenomenon could only occur when the charged jet was not “dry” enough prior to its deposition on the target, causing some parts of the partially discharged jet to contract to form beads. As soon as the collected jet was “dry” enough, contraction cannot occur any longer, thus leaving only beaded fibers on the target. The “dryness” of the charged jet is controlled mainly by the amount of the solvent that can evaporate during the flight of the charged jet to the target. The amount of the evaporating solvent is determined by a number of factors: e.g. the boiling point of the solvent, the initial concentration of the solution, the solution and the ambient temperatures, the diameter of the charged jet which continuously decreases during its flight to the target, and the total path length that the charged jet travels from the nozzle to the target which significantly depends on the extent of the bending instability^[9,10] that occurs.

The fact that beads along the fibers were observed at the concentration of 22% w/v and, with further increasing the concentration of the solutions to 34% w/v, the amount of beads decreased and the beads appeared to be more elongated in shape supported the above-mentioned postulation on the formation of beads. With increasing concentration (within the range of 22 to 34% w/v), the initial amount of the solvents in a small segment of a charged jet decreased, rendering the charged jet to “dry” much easier. However, the increased concentration enabled the charged jet to withstand larger stretching force (from the Coulombic repulsion), resulting in the observed larger diameter of the charged jet (ultimately, the as-spun fibers). In addition, the observed larger diameter had an adverse effect on the extent of the bending instability which determined the total path length of a jet segment during its

flight to the grounded target. It should be noted that the longer path length means the higher probability for the jet segment to thin down as a result of the Coulombic repulsion.

Figure 3 illustrates the appearance of non-woven PA-6-17 webs on the grounded target. The concentrations of the solutions were 30, 38, 42, and 46% w/v, respectively, while the applied electrostatic field and the collection time were fixed at 21 kV/10 cm and 30 seconds, respectively. Obviously, the diameter of the non-woven webs obtained decreased, while the areal density of the obtained fibers increased, with increasing concentration of the solutions. Due to an increase in the viscosity, the ejected, charged jet from solutions of higher concentrations had greater resistance towards the thinning of its diameter. This caused the charged jet to travel in a straight trajectory for a longer distance before undergoing a bending instability^[9,10] and this is postulated to be the main reason for the observed smaller diameter of the non-woven webs collected at higher concentrations (see Figure 3). The longer distance of the straight trajectory with increasing concentration of PA-6-17 is in excellent agreement with an earlier report in a previous work^[20] on poly(2-hydroxyethyl methacrylate) and polystyrene. Both the increase in the viscoelastic force and the decrease in the total path length of a jet segment resulted in an increase in the diameter of the as-spun fibers obtained from solutions of higher concentrations (see Figure 2e to h).

In order to quantitatively illustrate the effect of solution concentration on the diameters of the ultrafine PA-6-17 fibers, as-spun fibers with small amount of beads present or no beads at all were measured for their diameter and the concentration of the solutions that resulted in such fibers was in the range of 30 to 46% w/v (equivalent to the viscosity in the range of 738 to 3992 cp). Selected micrographs of some of these fibers are shown in Figure 2e to h at the magnification of 10000 \times . Obviously from these micrographs, the diameters of the obtained fibers were found to increase with increasing solution concentration, as previously mentioned. Figure 4 shows plots of the average diameter of the as-spun fibers from solutions of PA-6-17 in various concentrations ranging from 30 to 46% w/v as a function of the solution concentration and the solution viscosity. Apparently, the average fiber diameter was found to increase monotonically from ca. 66 nm at 30% w/v (equivalent to the

viscosity of 738 cp) to ca. 232 nm at 46% w/v (equivalent to the viscosity of 3992 cp). Other studies found the average diameter of the as-spun PA-6 to be in the range of 100 to 500 nm.^[21,22] According to Figure 4, it was found that the relationships between the average fiber diameter and the solution concentration and between the average fiber diameter and the solution viscosity could be best described by an exponential growth equation (see equations in Figure 4). It should be noted here again that the selection of the exponential growth equation to describe the data was based solely on the quality of the fitting that the equation provided.

3.3. Effect of PA-6 average molecular weight

Figure 5 shows a selected series of scanning electron micrographs portraying the effect of the average molecular weight of PA-6 on morphological appearance of the as-spun materials obtained from three different concentrations (i.e. 10, 20, and 34% w/v). Obviously, at 10% w/v, a large number of small droplets were present in the micrographs for PA-6-17 and PA-6-20 (see Figure 5a and d), while a mixture of small droplets and smooth fibers was obtained for PA-6-32 (see Figure 5g). At 20% w/v, a mixture of small droplets and smooth fibers was present in the micrographs for PA-6-17 and PA-6-20 (see Figure 5b and e), while only smooth fibers were observed in the case of PA-6-32 (see Figure 5h). With further increasing the solution concentration to 30% w/v, only smooth fibers were observed for all of the PA-6 resins investigated (see Figure 5c, f, and i). It is apparent, based on the micrographs shown in Figure 5, that, for a given PA-6 resin, the tendency for the observation of droplets or beaded fibers was found to decrease, while the diameters of the smooth fibers obtained were found to increase, with increasing concentration of the solutions. The most likely explanation for such observation should be the much greater increase in the viscoelastic force as a result of the large increase in the degree of chain entanglements (due to the increase in the solution concentration, hence the increase in the solution viscosity) in comparison with the Coulombic force.

The critical concentrations for the observation of beaded fibers (in combination with some smooth fibers, but without the presence of discrete droplets) and of smooth fibers (without the presence of beaded fibers) for the three resins were quite different. Specifically, the critical concentration for the observation of beaded

fibers for PA-6-17 was 22% w/v, for PA-6-20 was 20% w/v, and for PA-6-32 was 14% w/v, while the critical concentration for the observation of smooth fibers for PA-6-17 was 34% w/v, for PA-6-20 was 34% w/v, and for PA-6-32 was 22% w/v. Interestingly, despite the somewhat difference in these critical concentrations, the critical viscosities for the observation of beaded fibers and of smooth fibers for the three resins were quite comparable. Particularly, the critical concentration for the observation of beaded fibers for PA-6-17 was 277 cp, for PA-6-20 was 225 cp, and for PA-6-32 was 256 cp, while the critical concentration for the observation of smooth fibers for PA-6-17 was 1332 cp, for PA-6-20 was 1390 cp, and for PA-6-32 was 1150 cp. Based on the results obtained, the most important parameter determining the morphological appearance of the electrospun fibers should be viscosity, rather than the concentration of the solution.

Figure 6 illustrates average diameter of as-spun PA-6-17, PA-6-20, and PA-6-32 fibers plotted as function of both the concentration and the viscosity of the solutions. It should be noted that the diameter of the obtained fibers were measured from micrographs showing the as-spun fibers with small amount of beads present or no beads at all. In both PA-6-17 and PA-6-20, the measurable concentration of the solutions was in the range of 30 to 46% w/v (equivalent to the viscosity in the range of 738 to 3992 cp for PA-6-17 and of 849 to 4058 cp for PA-6-20), while, in PA-6-32, the measurable concentration range was from 20 to 30% w/v (equivalent to the viscosity in the range of 795 to 3867 cp). For a given PA-6 resin, the average fiber diameter was found to monotonically increase with increasing both the concentration and the viscosity of the solutions. Specifically, the average fiber diameter for PA-6-17 was found to increase from ca. 66 to 232 nm, for PA-6-20 from ca. 92 to 395 nm, and for PA-6-32 from ca. 82 to 174 nm. It was also shown in Figure 6a that the average fiber diameter obtained for each resin exhibited a finite relationship with the solution concentration, which can be approximated by an exponential growth equation (see equations in Figure 6a).

Instead of plotting the average fiber diameter for each resin as a function of the solution concentration, the average fiber diameters for all of the resins were plotted as a function of the solution viscosity in Figure 6b. Apparently, the average fiber diameters for all of the resins exhibited a common relationship with the solution

viscosity, especially within the viscosity range of 738 to 2191 cp. As it was shown for the case of PA-6-17 resin in Figure 4, the common relationship between average fiber diameters for all of the resins investigated and the respective solution viscosity could be numerically fitted to an exponential growth equation of the form:

$$\text{Average fiber diameter (nm)} = 88.7 + 0.804 \exp(0.00137 \times \text{Viscosity (cp)}). \quad (1)$$

3.4. Effect of solution temperature

In order to illustrate the effect of solution temperature on morphological appearance of the as-spun PA-6 fibers, solution of PA-6-32 in 85% v/v formic acid was prepared at the concentration of 20% w/v. Prior to electrospinning, the as-prepared solution was stocked in a home-made double-chambered syringe and its temperature was equilibrated by warm water, the temperature of which was set at 30, 40, 50, or 60°C. Some physical properties (i.e. viscosity, surface tension, and conductivity) of the as-prepared solution at different temperatures investigated were measured and the results are summarized in Table 1. It should be noted that the viscosity and the surface tension of the solution measured at room temperature were 795 cp and 43.1 mN/m, respectively. According to Table 1, all of the solution property values were found to monotonically decrease with an increase in the solution temperature.

The as-spun PA-6-32 fibers obtained from the solutions of different temperatures were found to be similar in their morphology which was a combination of beaded and smooth fibers. The only difference in the morphology of the fibers obtained was in the average fiber diameter, which was found to decrease from ca. 98 nm at the solution temperature of 30°C to ca. 90 nm at the solution temperature of 60°C (see Figure 7 for examples). Since the concentration of the solution was fixed, elevation of the solution temperature resulted in the expansion of the polymer molecules, leading to the reduction in the degree of chain entanglements, hence the reduction in the solution viscosity. The reduction in the viscosity means the reduction in the viscoelastic force to counter the Coulombic stretching force, which finally resulted in the observed reduction in the fiber diameters.

Besides the reduction in the fiber diameters, the micrographs shown in Figure 7 also suggest that the number of fibers depositing on the target was found to increase with increasing solution temperature. For a fixed mass throughput, the decrease in the average fiber diameter implied an increase in the total length of the as-spun fibers. For a fixed deposition period, the increase in the total length of the fibers resulted in an increase in the number of fibers depositing on the target. In working with the electrospinning of segmented polyurethaneurea (PUU) in dimethylformamide (DMF) at elevated temperatures of the solutions, Demir and co-workers^[16] observed an increase in the deposition rate of the fibers as a function of the solution temperature, which is in accord with what has been observed in this work.

3.5. Effect of solvent system

In order to investigate the effect of solvent system on morphological appearance of the as-spun PA-6 fibers, solutions of PA-6-20 were prepared by dissolving the pellets in mixed solvents of 85% v/v formic acid and *m*-cresol in various compositional ratios between formic acid and *m*-cresol of 90:10, 80:20, 70:30, 60:40, and 50:50 v/v prior to electrospinning. Some physical properties (i.e. viscosity, surface tension, and conductivity) of the as-prepared solutions were measured and the results are summarized in Table 2. It should be noted that the property values for the solution in 85% v/v formic acid were also listed for comparison. Interestingly, the viscosity of the solutions was found to markedly increase, the surface tension to decrease slight, and the conductivity to decrease appreciably, with addition and increasing amount of *m*-cresol. The decrease in the conductivity of the solutions with increasing amount of *m*-cresol could be a result of the much lower dielectric constant of *m*-cresol (i.e. 11.5 at 23.9°C^[23]) in comparison with that of formic acid (i.e. 58.5 at 15.6°C^[23]).

Figure 8 shows selected scanning electron micrographs of as-spun fibers obtained from the solutions of PA-6-20 in a mixed solvent of 85% v/v formic acid and *m*-cresol in various compositional ratios of 90:10, 80:20, and 60:40 v/v. The micrograph exhibiting the as-spun fibers obtained from the solution of PA-6-20 in *m*-

cresol is also shown for comparison (see Figure 8d). While the 32% w/v solution of PA-6-20 in 85% v/v formic acid produced smooth fibers, the 32% w/v solution of PA-6-20 in *m*-cresol produced nothing but blobs of the solution on the collector. The most likely explanation for such observation may be due to the much higher boiling point of *m*-cresol (i.e. 202°C^[24]) in comparison with that of formic acid (i.e. 101°C^[25]). With such a high boiling point, the charged jet from the solution of PA-6-20 in *m*-cresol did not have enough time to "dry" prior to depositing on the target. The "rather wet" depositing jet then fused with adjacent depositing jets to form blobs of the solution observed.

In the mixed solvent system, smooth and separate fibers were obtained when the content of *m*-cresol was varied between 10 and 30% v/v and further increasing in the *m*-cresol content to 40 and 50% v/v resulted in the observation of smooth fibers that were fused to one another at touching points (see Figure 8). The occurrence of the fused fiber morphology should be due to the high boiling point of *m*-cresol. Evidently, the diameters of the obtained fibers were found to increase with increasing amount of *m*-cresol added. Specifically, the average fiber diameter increased from ca. 94 nm for PA-6-20 solution in 85% v/v formic acid to ca. 201 nm for PA-6-20 solution in a mixed solvent of 85% v/v formic acid and *m*-cresol at the compositional ratio of 50:50 v/v. The increase in the average fiber diameter with increasing *m*-cresol content could be due to both the increase in the solution viscosity and the decrease in the solution conductivity with increasing *m*-cresol content. This simply means that, at higher *m*-cresol contents, the Coulombic stretching force decreased, while the viscoelastic force which counters the Coulombic stretching force increased, resulting in an increase in the diameters of the as-spun fibers.

3.6. Effect of salt addition

In order to investigate the effect of salt addition on morphological appearance of the obtained electrospun fibers, various types of inorganic salt (i.e. NaCl, LiCl, and MgCl₂) in the amount ranging from 1 to 5% w/v were added to 32% w/v PA-6-20 solution in 85% v/v formic acid. The 5% w/v content of the inorganic salt was the dissolution limit that these salts could be dissolved in the 32% w/v PA-6-20

solution. Table 3 summarizes the viscosity, surface tension, and conductivity values of the as-prepared solutions as well as the diameters of the obtained electrospun fibers. It should be noted that the viscosity, surface tension, and conductivity values for the 32% w/v PA-6-20 solution in 85% v/v formic acid were ca. 1160 cp, 44 mN/m, and 4 mS/cm, respectively. Obviously, addition of these inorganic salts resulted in the reduction in the viscosity values and the increase in the conductivity values, while they seemed not to affect the surface tension of the obtained solutions.

According to Table 3, the viscosity values of PA-6-20 solutions with addition of NaCl and LiCl salts were found to increase with increasing content of the added salts, while those of the solution with addition of MgCl₂ seems not to have a finite relationship with the salt content. In addition, the conductivity values of the solutions were found to increase monotonically with an increase in the salt content. For NaCl- and LiCl-added solutions, the increase in the viscosity values suggests an increase in the viscoelastic force counteracting the Coulombic stretching force with increasing salt content, while, for all of the solutions investigated, the increase in the conductivity values suggests an increase in both the electrostatic and the Coulombic forces with increasing amount of the added salts. Intuitively, the increase in the Coulombic stretching force should result in the reduction in the obtained fiber diameters (provided that the viscoelastic force was, more or less, constant), but the results summarized in Table 3 suggest otherwise. The otherwise increase in the fiber diameters with increasing the amount of salts added could be a result of the increase in the viscoelastic force (i.e. for fibers obtained from NaCl- and LiCl-added solutions) and the increase in the mass flow (due to the increase in the electrostatic force acting on the jet segments). Demir and co-workers^[16] also reported an increase in the mass flow with addition of triethylbenzylammonium chloride in a solution of PUU in DMF.

4. CONCLUSIONS

In the present contribution, the effects of solution conditions on morphological appearance and average diameter of the as-spun polyamide-6 (PA-6) fibers were thoroughly investigated using optical scanning (OS) and scanning electron microscopy (SEM) techniques. An increase in the solution concentration

caused a marked increase in the solution viscosity and the relationship between the solution viscosity and the solution concentration could be approximated by an exponential growth equation. At low solution viscosities, only small droplets were present. At slightly higher viscosities, a combination of small droplets and smooth fibers was obtained. At some critical viscosities, droplets disappeared altogether, leaving only beaded and smooth fibers on the collective target. Further increasing the solution viscosity resulted in the reduced number of beads and the increased fiber diameters. At high enough solution viscosities, only smooth fibers were present.

At a given concentration, fibers obtained from PA-6 of higher molecular weights appeared to be larger in diameter, but it was observed that the average diameters of the fibers obtained from PA-6 of different molecular weights exhibited a common relationship with the viscosities of the solutions which could be approximated by an exponential growth equation. An increase in the temperature of the solution during electrospinning resulted in a decrease in the fiber diameters, but resulted in an increase in the deposition rate. Mixing *m*-cresol with formic acid to serve as a mixed solvent for PA-6 caused the resulting solutions to have higher viscosity values which resulted in the larger fiber diameters observed. Lastly, addition of some inorganic salts to the solution resulted in an increase in the conductivity values, which, in turn, caused the fiber diameters to increase due to the large increase in the mass flow.

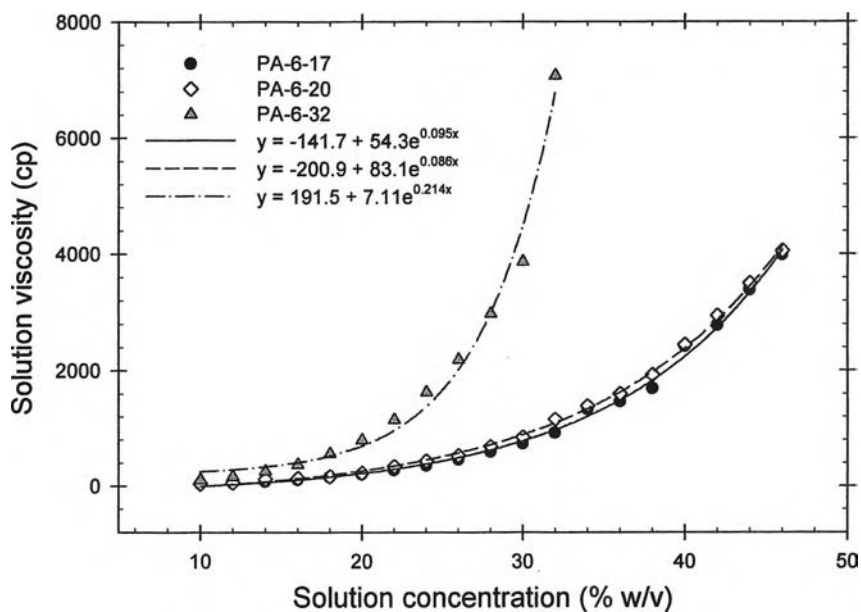
ACKNOWLEDGEMENTS

The authors acknowledge partial supports received from the National Research Council of Thailand (contract grant number: 03009582-0002), Chulalongkorn University (through invention and research grants from the Ratchadapesek Somphot Endowment Fund), the Petroleum and Petrochemical Technology Consortium [through a Thai governmental loan from the Asian Development Bank (ADB)], and the Petroleum and Petrochemical College (PPC), Chulalongkorn University. Helpful discussion with Dr. Ratthapol Rangkupan of the Metallurgy and Materials Science Research Institute (MMRI), Chulalongkorn University is also gratefully acknowledged.

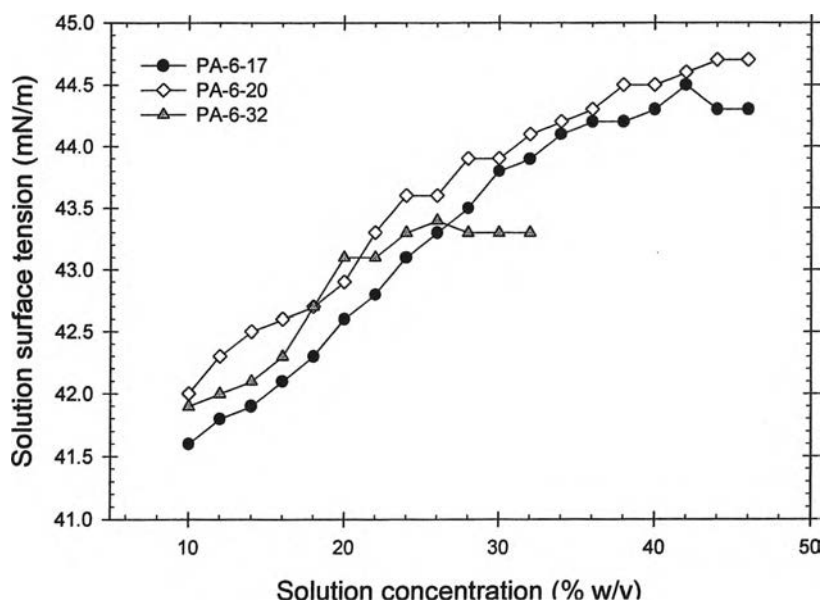
REFERENCES

- [1] J. Cross, “*Electrostatics: Principles, Problems, and Applications*”, Adam Hilger, Bristol 1987.
- [2] US Patent 1,975,504 (1934), inv. A. Formhals.
- [3] US Patent 2,160,962 (1939), inv. A. Formhals.
- [4] US Patent 2,187,306 (1940), inv. A. Formhals.
- [5] US Patent 2,323,025 (1943), inv. A. Formhals.
- [6] US Patent 2,349,950 (1944), inv. A. Formhals.
- [7] Z. M. Huang, Y. Z. Zhang, M. Kotaki, S. Ramakrishna, *Composites Science and Technology* **2003**, *63*, 2223.
- [8] L. Wannatong, A. Sirivat, P. Supaphol, *Polymer International*, in press.
- [9] D. H. Reneker, I. Chun, *Nanotechnology* **1996**, *7*, 216.
- [10] D. H. Reneker, A. L. Yarin, H. Fong, S. Koombhongse, *Journal of Applied Physics* **2000**, *87*, 4531.
- [11] J. Doshi, D. H. Reneker, *Journal of Electrostatics* **1995**, *35*, 151.
- [12] P. K. Baumgarten, *Journal of Colloid and Interface Science* **1971**, *36*, 71.
- [13] H. Fong, I. Chun, D. H. Reneker, *Polymer* **1999**, *40*, 4585.
- [14] J. M. Deitzel, J. Kleinmeyer, D. Harris, and N. C. Beck Tan, *Polymer* **2001**, *42*, 261.
- [15] C. J. Buchko, L. C. Chen, Y. Shen, D. C. Martin, *Polymer* **1999**, *40*, 7397.
- [16] M. M. Demir, I. Yilgor, E. Yilgor, B. Erman, *Polymer* **2002**, *43*, 3303.
- [17] X. Zong, K. Kim, D. Fang, S. Ran, B. S. Hsiao, B. Chu, *Polymer* **2002**, *43*, 4403.
- [18] H. Liu, Y. L. Hsieh, *Journal of Polymer Science: B. Polymer Physics* **2002**, *40*, 2119.
- [19] K. H. Lee, H. Y. Kim, M. S. Khil, Y. M. Ra, D. R. Lee, *Polymer* **2003**, *44*, 1287.
- [20] S. Koombhongse, “*PhD Dissertation*”, University of Akron, Akron, Ohio (2001).
- [21] X. Fang, “*PhD Dissertation*”, University of Akron, Akron, Ohio (1997).
- [22] H. Fong, W. Liu, C. Wang, R. Vaia, *Polymer* **2002**, *43*, 775.

- [23] http://www.orioninstruments.com/html/dielectric_constants.asp
- [24] <http://www.jtbaker.com/msds/englishhtml/c5456.htm>
- [25] <http://www.jtbaker.com/msds/englishhtml/f5956.htm>



(a)



(b)

Figure 1. (a) Viscosity; (b) surface tension; and (c) conductivity as a function of polyamide-6 concentration for solutions of polyamide-6 of three different weight-average molecular weights in 85% v/v formic acid.

I 22242995

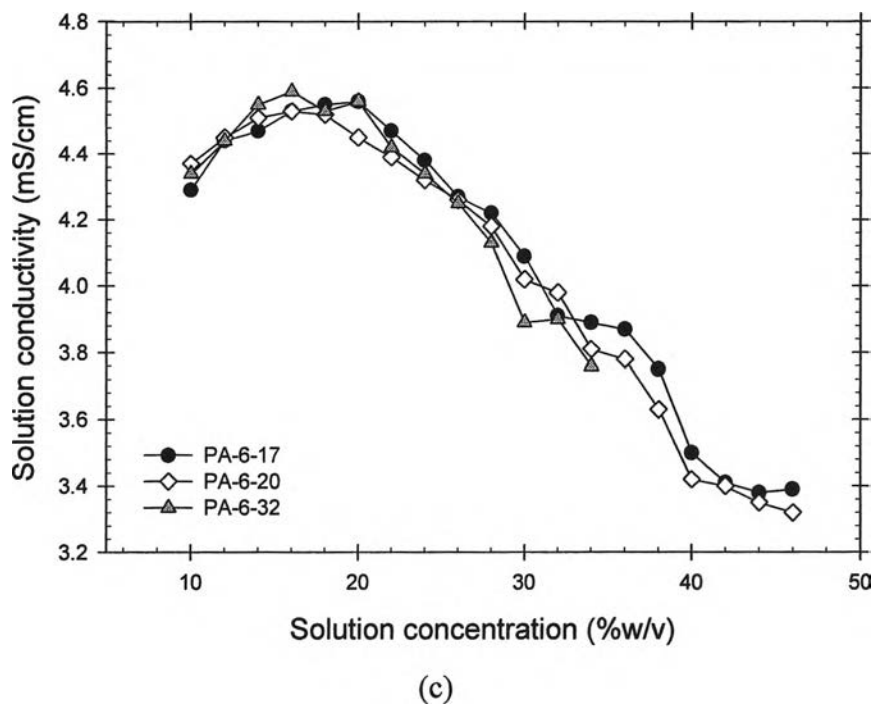


Figure 1. (cont.) (a) Viscosity; (b) surface tension; and (c) conductivity as a function of polyamide-6 concentration for solutions of polyamide-6 of three different weight-average molecular weights in 85% v/v formic acid.

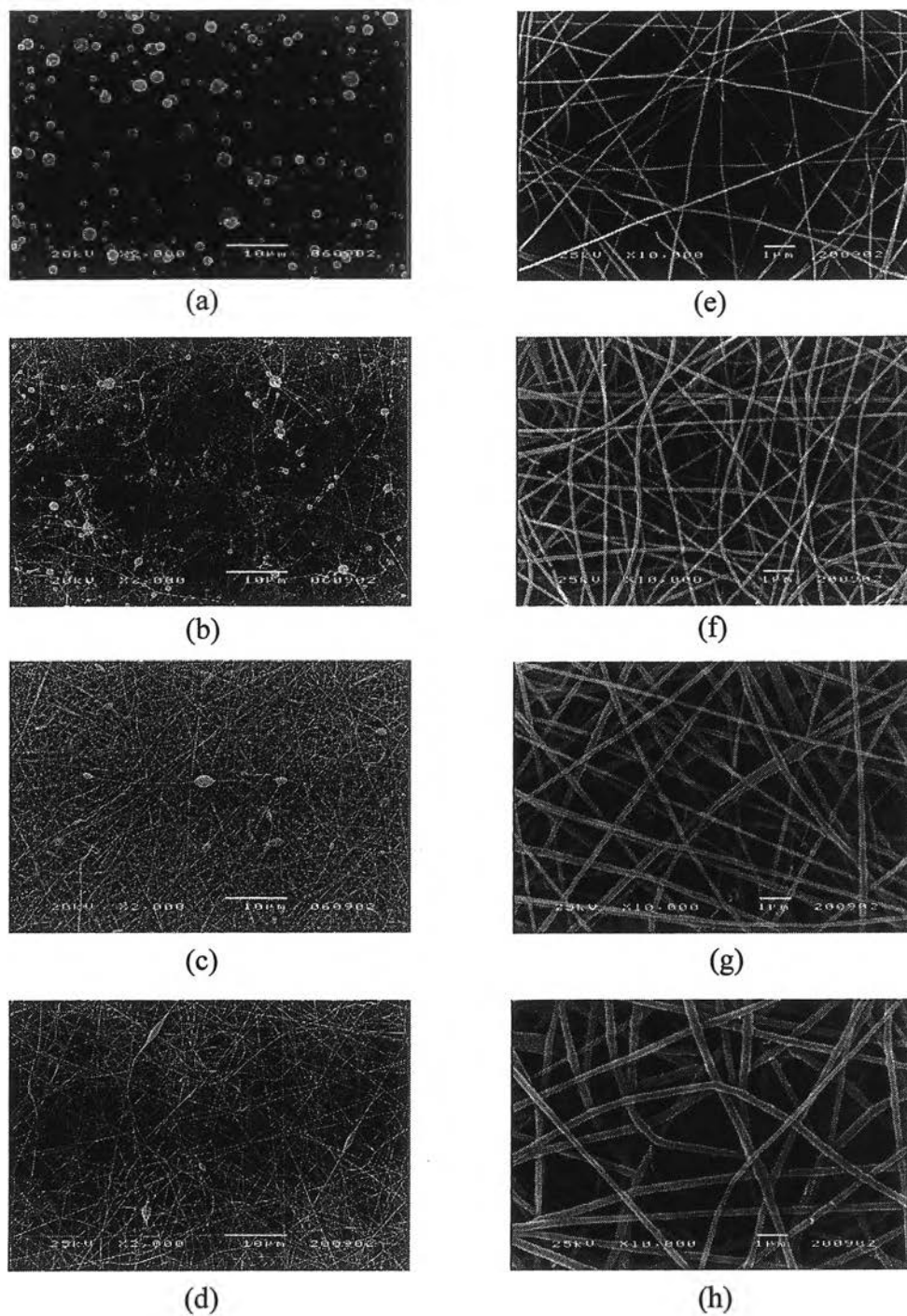


Figure 2. Scanning electron micrographs of electrospun materials obtained from solutions of PA-6-17 in 85% v/v formic acid at the concentrations: a) 14; b) 20; c) 24; and d) 32% w/v (the magnification = 2000 \times and the scale bar = 10 μ m) and at the concentrations: e) 32; f) 38; g) 42; and h) 46% w/v (the magnification = 10000 \times and the scale bar = 1 μ m).

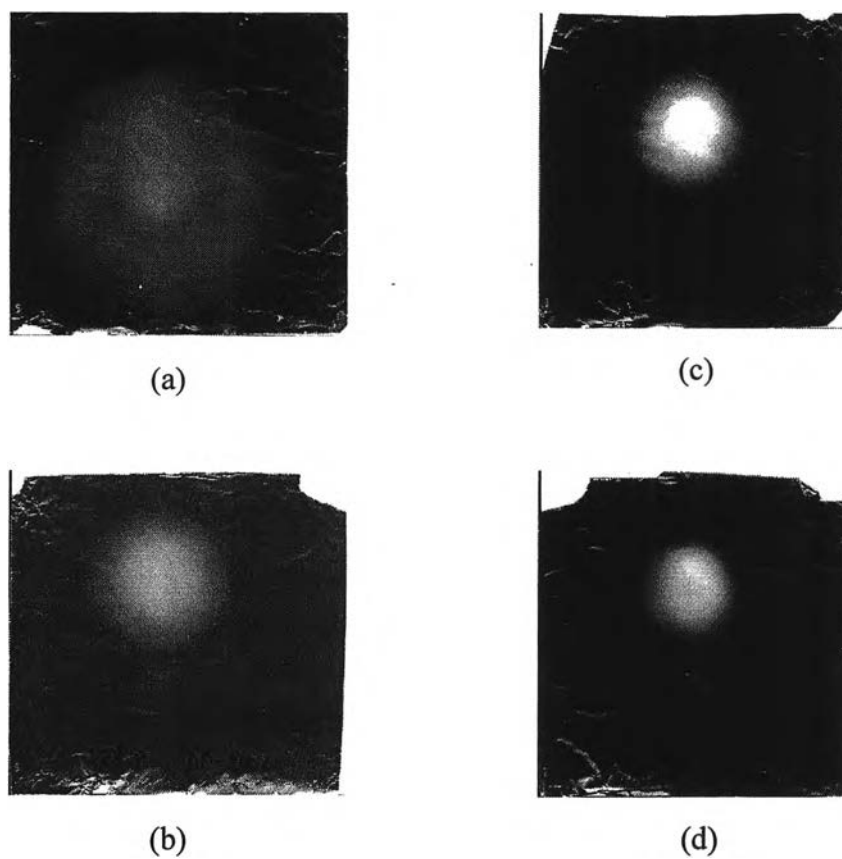


Figure 3. Optical scanning photographs of non-woven web of polyamide-6 fibers from solutions of PA-6-17 in 85% v/v formic acid at the concentrations: a) 32; b) 38; c) 42; and d) 46% w/v. The collection time was fixed at 30 seconds.

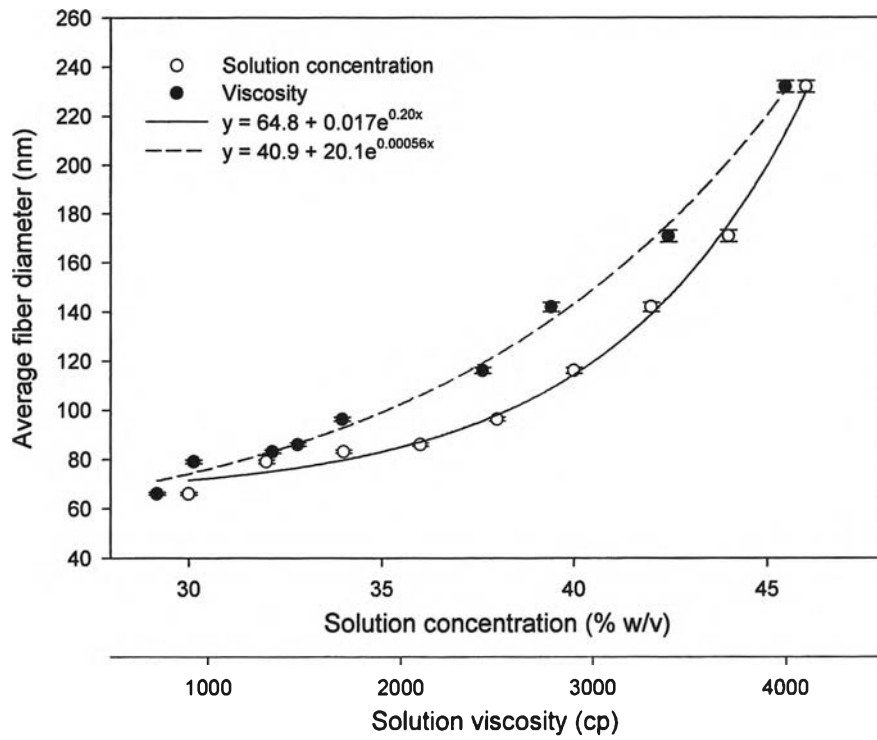


Figure 4. Average diameter of as-spun PA-6-17 fibers plotted as a function of the concentration and the viscosity of the solutions.

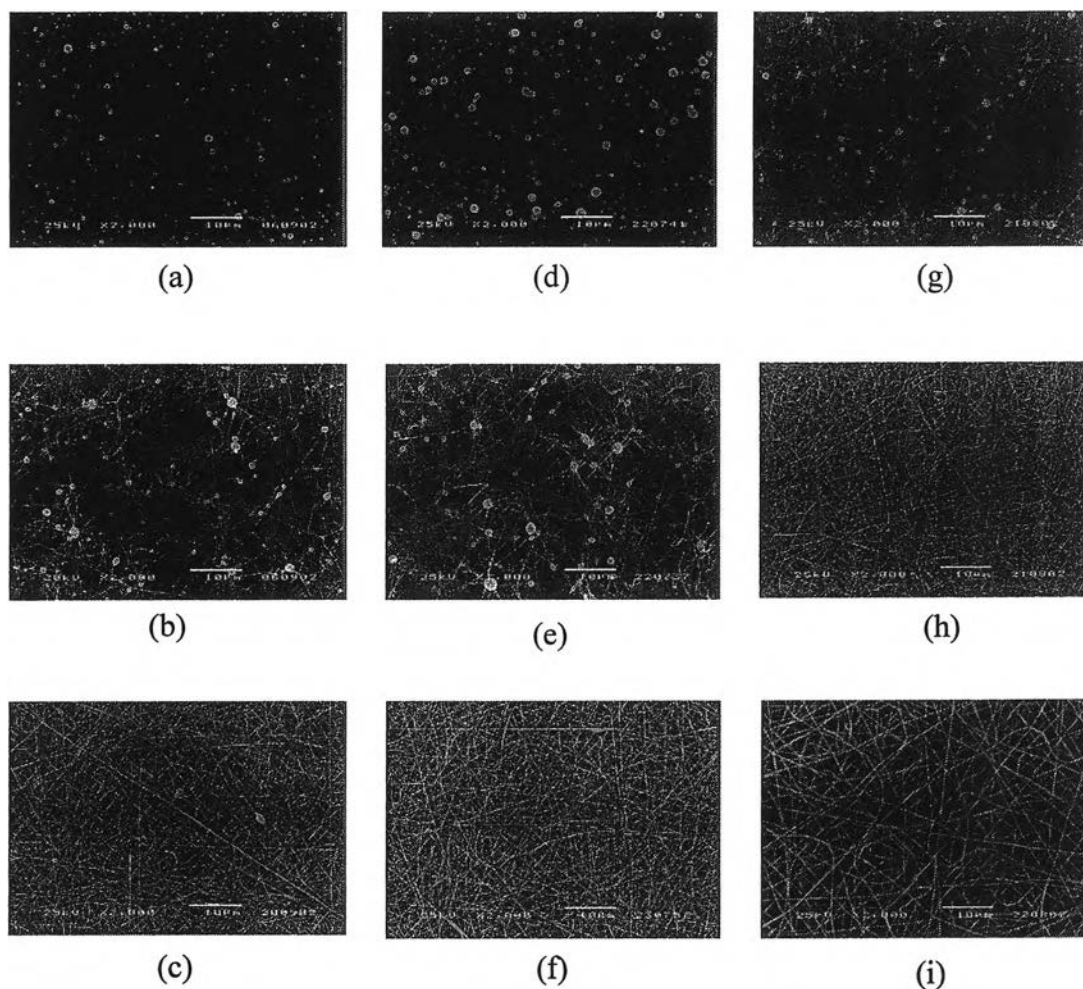
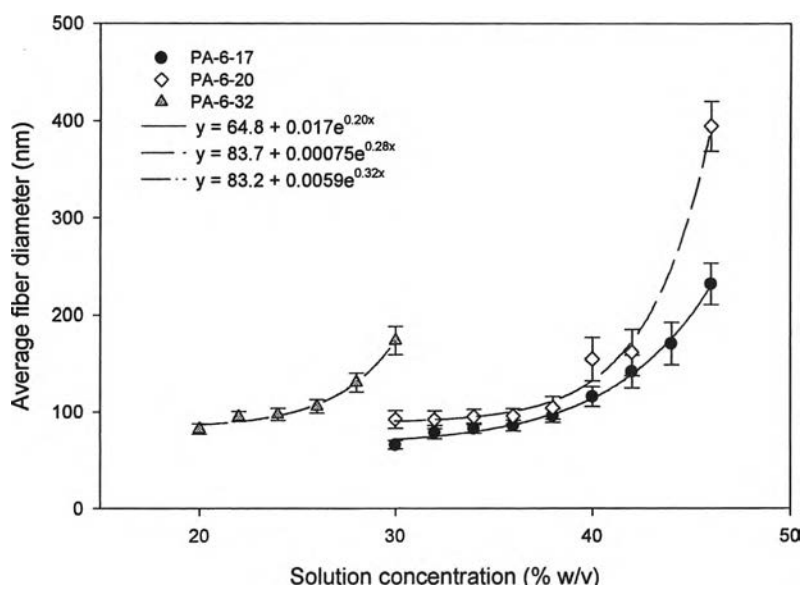
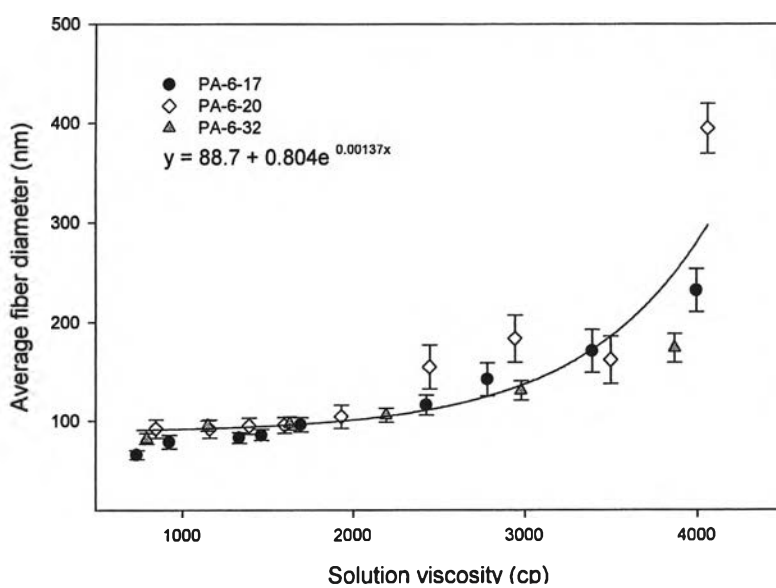


Figure 5. Scanning electron micrographs of electrospun materials obtained from solutions of PA-6-17 in 85% v/v formic acid at the concentrations: a) 10; b) 20; and c) 34% w/v, from solutions of PA-6-20 in 85% v/v formic acid at the concentrations: d) 10; e) 20; and f) 34% w/v, and from solutions of PA-6-32 in 85% v/v formic acid at the concentrations: g) 10; h) 20; and i) 34% w/v (the magnification = 2000 \times and the scale bar = 10 μ m).

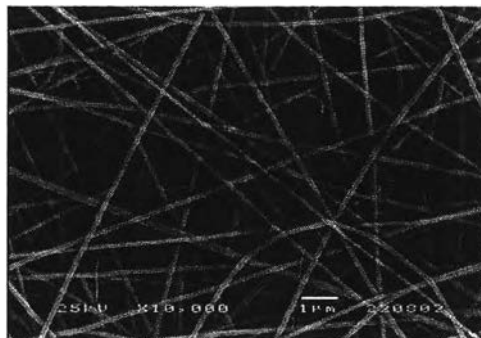


(a)

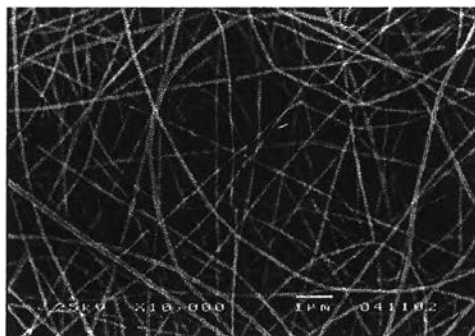


(b)

Figure 6. Average diameter of as-spun PA-6-17, PA-6-20, and PA-6-32 fibers plotted as a function of (a) the concentration and (b) the viscosity of the solutions.



(a)



(b)

Figure 7. Scanning electron micrographs of electrospun fibers obtained from solutions of PA-6-32 at the concentration of 20% w/v in 85% v/v formic acid at solution temperatures: a) 30; and b) 60°C (the magnification = 10000× and the scale bar = 1 µm).

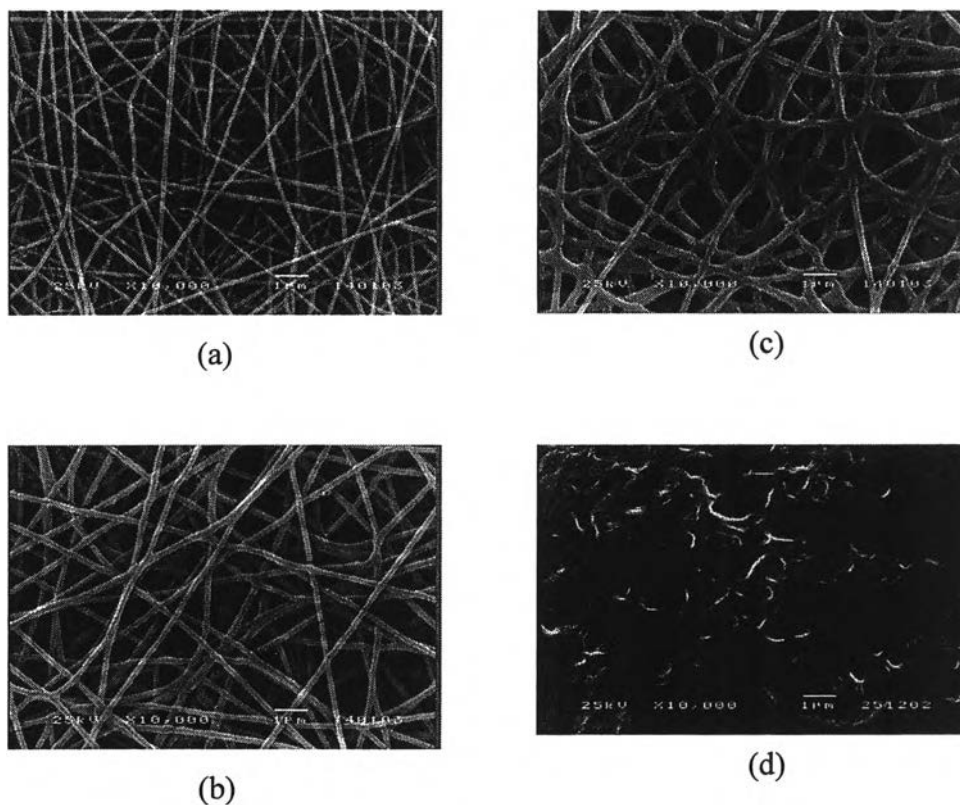


Figure 8. Scanning electron micrographs of electrospun fibers obtained from solutions of PA-6-20 at the concentration of 32% w/v in a mixed solvent of 85% v/v formic acid and *m*-cresol in various compositional ratios: a) 90:10; b) 80:20; and c) 60:40 v/v and d) from solution of PA-6-20 at the concentration of 32% w/v in *m*-cresol (the magnification = 10000× and the scale bar = 1 μm).

Table 1. Viscosity, surface tension, and conductivity of 20% w/v polyamide-6 ($M_w = 32,000$ Da) solutions in 85% v/v formic acid at different temperatures and diameter of the resulting as-spun fibers.

Solution temperature (°C)	Viscosity (cp)	Surface tension (mN/m)	Conductivity (mS/cm)	Fiber diameter (nm)
30	517	43.2	4.2	98.3 ± 8.2
40	387	42.3	3.9	94.0 ± 6.3
50	284	41.8	3.8	91.8 ± 7.2
60	212	41.1	3.4	89.7 ± 5.6

Table 2. Viscosity, surface tension, and conductivity of 32% w/v polyamide-6 ($M_w = 20,000$ Da) solutions in mixed solvent of 85% v/v formic acid and *m*-cresol in various compositional ratios (v/v) and diameter of the resulting as-spun fibers.

Mixed solvent of formic acid and <i>m</i> -cresol in various compositional ratios (v/v)	Viscosity (cp)	Surface tension (mN/m)	Conductivity (mS/cm)	Fiber diameter (nm)
100/0	1160	44.1	4.0	93.5 ± 6.0
90/10	1709	42.4	2.9	110.4 ± 6.9
80/20	2104	41.3	2.1	166.1 ± 10.5
70/30	3127	40.6	1.4	170.3 ± 9.8
60/40	4075	39.8	0.8	188.6 ± 17.3
50/50	4550	39.3	0.4	200.5 ± 13.2

Table 3. Viscosity, surface tension, and conductivity of 32% w/v polyamide-6 ($M_w = 20,000$ Da) solutions in 85% v/v formic acid with addition of NaCl, LiCl, or $MgCl_2$ salt in various amount ranging from 1 to 5% w/v and diameter of the resulting as-spun fibers.

Type of salt added	Amount of salt added (% w/v, mole $\times 10^{-2}$)	Viscosity (cp)	Surface tension (mN/m)	Conductivity (mS/cm)	Fiber diameter (nm)
NaCl	1 (0.43)	558	43.5	6.2	98.6 ± 7.4
	2 (0.86)	576	43.9	8.0	101.5 ± 6.0
	3 (1.28)	599	44.0	9.6	114.3 ± 7.1
	4 (1.71)	556	44.9	11.1	124.8 ± 7.3
	5 (2.14)	694	44.9	12.2	134.2 ± 13.3
LiCl	1 (0.59)	614	43.8	6.3	105.4 ± 9.0
	2 (1.18)	683	43.9	8.5	138.2 ± 11.6
	3 (1.76)	708	43.8	10.3	147.8 ± 16.5
	4 (2.36)	783	44.3	11.9	168.7 ± 15.0
	5 (2.95)	871	45.0	13.1	168.3 ± 15.1
$MgCl_2$	1 (0.26)	639	43.8	5.0	99.4 ± 9.1
	2 (0.53)	644	43.9	5.8	102.7 ± 7.8
	3 (0.79)	604	44.1	6.5	118.8 ± 9.9
	4 (1.05)	618	44.1	7.2	127.7 ± 11.6
	5 (1.57)	634	44.2	8.3	131.7 ± 12.3